

# Time-dependent stimulation by aldosterone of blocker-sensitive ENaCs in A6 epithelia

SANDY I. HELMAN,<sup>1</sup> XUEHONG LIU,<sup>1</sup> KIERON BALDWIN,<sup>3</sup>  
BONNIE L. BLAZER-YOST,<sup>2</sup> AND WILLEM J. ELS<sup>3</sup>

<sup>1</sup>Department of Molecular and Integrative Physiology, University of Illinois at Urbana-Champaign, Urbana, Illinois 61801; <sup>2</sup>Department of Biology, Indiana University-Purdue University at Indianapolis and Veterans Affairs Medical Center, Indianapolis, Indiana 46202; and <sup>3</sup>Department of Anatomy and Cell Biology, University of Cape Town Medical School, Cape Town, South Africa

**Helman, Sandy I., Xuehong Liu, Kieron Baldwin, Bonnie L. Blazer-Yost, and Willem J. Els.** Time-dependent stimulation by aldosterone of blocker-sensitive ENaCs in A6 epithelia. *Am. J. Physiol. Cell Physiol.* 274 (C947–C957, 1998).—To study and define the early time-dependent response ( $\leq 6$  h) of blocker-sensitive epithelial  $\text{Na}^+$  channels (ENaCs) to stimulation of  $\text{Na}^+$  transport by aldosterone, we used a new modified method of blocker-induced noise analysis to determine the changes of single-channel current ( $i_{\text{Na}}$ ) channel open probability ( $P_o$ ), and channel density ( $N_T$ ) under transient conditions of transport as measured by macroscopic short-circuit currents ( $I_{\text{sc}}$ ). In three groups of experiments in which spontaneous baseline rates of transport averaged 1.06, 5.40, and 15.14  $\mu\text{A}/\text{cm}^2$ , stimulation of transport occurred due to increase of blocker-sensitive channels.  $N_T$  varied linearly over a 70-fold range of transport (0.5–35  $\mu\text{A}/\text{cm}^2$ ). Relatively small and slow time-dependent but aldosterone-independent decreases of  $P_o$  occurred during control (10–20% over 2 h) and aldosterone experimental periods (10–30% over 6 h). When the  $P_o$  of control and aldosterone-treated tissues was examined over the 70-fold extended range of  $\text{Na}^+$  transport,  $P_o$  was observed to vary inversely with  $I_{\text{sc}}$ , falling from  $\sim 0.5$  to  $\sim 0.15$  at the highest rates of  $\text{Na}^+$  transport or  $\sim 25\%$  per 3-fold increase of transport. Because decreases of  $P_o$  from any source cannot explain stimulation of transport by aldosterone, it is concluded that the early time-dependent stimulation of  $\text{Na}^+$  transport in A6 epithelia is due exclusively to increase of apical membrane  $N_T$ .

electrophysiology; epithelial sodium channels; tissue culture; cortical collecting ducts; kidney; noise analysis; amiloride

APICAL MEMBRANES OF A variety of tight epithelia express epithelial  $\text{Na}^+$  channels (ENaCs) that function in regulating the rate of  $\text{Na}^+$  entry into the cells and its subsequent transport through basolateral membranes. Aldosterone is known to play a key role in regulation of baseline rates of transport at both surfaces of the cells (Refs. 3, 5, 18, 20, 24, 27, 28 and references therein), acting to modulate apical membrane transport by way of change of the permeability to  $\text{Na}^+$ . To understand the underlying mechanisms involved, it is necessary to distinguish between changes of permeability due to changes of channel density ( $N_T$ ) and changes of channel open probability ( $P_o$ ), as changes of either will lead to changes of the open channel density ( $N_o = P_o N_T$ ).

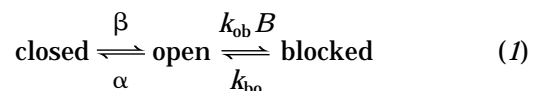
Aldosterone stimulates  $\text{Na}^+$  transport through at least two populations of channels (amiloride sensitive and insensitive) in native tissues like frog skin and toad urinary bladder and in cell-cultured A6 epithelia grown on permeable supports. Greater than 95% of transport

occurs through blocker-sensitive channels (16). Regardless of the origin of the pool of blocker-sensitive channels (activation of channels preexisting at the apical membranes and/or vesicle trafficking of channels to the membrane), it has been observed after chronic exposure to aldosterone ( $\sim 24$ – $48$  h) that the density of channels is increased with no measurable change of  $P_o$  (2, 23). In oocytes expressing ENaCs, aldosterone causes the appearance of channels with long open and closed times (7, 8) with  $P_o$  similar to those that have been observed by patch clamp of rat renal cortical collecting ducts (23) and A6 epithelia (9, 19, 21, 22) and by noise analysis of A6 epithelia (2, 13).

We have in the present set of experiments examined the early or initial response of A6 epithelia to aldosterone during the first 6 h following stimulation of transport by this steroid. Previous methods of noise analysis were limited to experiments done under conditions in which transport rates were stable (unchanged) for at least 30 min. We modified these methods so that channel densities and  $P_o$  could be measured noninvasively during transient changes of transport. Three groups of A6 epithelia were studied, with spontaneous baseline rates of  $\text{Na}^+$  transport averaging 1.06, 5.40, and 15.14  $\mu\text{A}/\text{cm}^2$ . The results of our experiments indicated that, despite large differences in baseline values of density of blocker-sensitive channels, stimulation of transport during the first 6 h could be attributed almost entirely to an increase of  $N_T$  with relatively minor compensatory decreases of single-channel current and channel  $P_o$ .

## Theoretical Considerations

*Equilibrium distribution of channels.* Spontaneous gating of blocker-sensitive ENaCs between open and closed states is sluggish, with mean open and closed times of several seconds. When a blocker inhibits the open state of the channels (2, 14), channels must redistribute among open, closed, and blocked states, giving rise to time-dependent changes of open channel density and hence  $\text{Na}^+$  entry into the cells. For a three-state scheme with open-to-closed, closed-to-open, blocker on, and blocker off rate coefficients,  $\alpha$ ,  $\beta$ ,  $k_{\text{ob}}$ , and  $k_{\text{bo}}$ , respectively, and blocker concentration  $B$



the equilibrium density of open channels at any  $B$  ( $N_o^B$ )

relative to the density of open channels in the absence of blocker ( $N_o$ ) is

$$\frac{N_o^B}{N_o} = [1 + P_o(B/K_B)]^{-1} \quad (2)$$

(14), where  $P_o = \beta/(\alpha + \beta)$  and the blocker equilibrium constant  $K_B = k_{bo}/k_{ob}$ . Because channels can be recruited from closed to open states, the fractional inhibition of open channel density and hence blocker-inhibitable transport is dependent on  $P_o$ . Under conditions in which single-channel currents in the absence of blocker ( $i_{Na}$ ) and in the presence of blocker ( $i_{Na}^B$ ) remain essentially constant, Eq. 2 can be rewritten as Eq. 3, since macroscopic current in the absence of blocker  $I_{Na} = i_{Na}N_o$  and macroscopic current in the presence of blocker  $I_{Na}^B = i_{Na}^BN_o^B$

$$\frac{I_{Na}^B}{I_{Na}} = [1 + P_o(B/K_B)]^{-1} \quad (3)$$

Hence  $P_o$  can be determined from the fractional inhibition of the blocker-sensitive short-circuit current when  $K_B$  is known. Because this relationship is not restricted to increases of blocker concentration from zero to  $B$ , it can be rewritten more generally for changes of solutions containing blocker concentrations  $B_1$  and  $B_2$  as

$$\frac{I_{Na}^{B_2}}{I_{Na}^{B_1}} = \frac{1 + P_o(B_1/K_B)}{1 + P_o(B_2/K_B)} \quad (4)$$

Solving for  $P_o$  and using the shortened notation  $I_{Na}^{B_2/B_1}$  to indicate the ratio of currents at  $B_2$  with respect to those at  $B_1$  gives

$$P_o = \left( \frac{1 - I_{Na}^{B_2/B_1}}{B_2 I_{Na}^{B_2/B_1} - B_1} \right) K_B \quad (5)$$

**Kinetics of channel redistribution.** With ideal instantaneous step increases of  $B$ , channels will redistribute between closed, open, and blocked states with time constants determined by the rate coefficients. For the blocker 6-chloro-3,5-diaminopyrazine-2-carboxamide (CDPC), for which  $k_{ob}$  and  $k_{bo}$  average near  $7 \text{ s}^{-1} \cdot \mu\text{M}^{-1}$  and  $210 \text{ s}^{-1}$ , respectively (Ref. 15; see also *CDPC rate coefficients*), the density of open channels will decrease promptly by 50% with a time constant near 2.5 ms when  $B$  is increased from 0 to  $B = K_B = 30 \mu\text{M}$ . With  $\alpha$  and  $\beta$  reflecting mean open and closed times of, for example, 3 s, open channel density will increase thereafter with a time constant of  $\sim 1.5$  s, as illustrated in Fig. 1A. The secondary long time constant for redistribution of the channels toward equilibrium will depend on the absolute values of  $\alpha$  and  $\beta$ , with the final equilibrium value of  $N_o^B/N_o$  determined by the  $P_o$ . For  $P_o$  of 0.1, 0.3, or 0.5 illustrated in Fig. 1A, the fractional  $N_o^B/N_o$  at equilibrium expressed as percentages are 90.1, 76.9, and 66.7%, respectively. It may be emphasized, as indicated in Fig. 1B, that the time constants for equilibration vary with  $(\alpha + \beta)^{-1}$  and the  $P_o$  is determined by  $\beta/(\alpha + \beta)$ . Thus  $P_o$  may appear to be

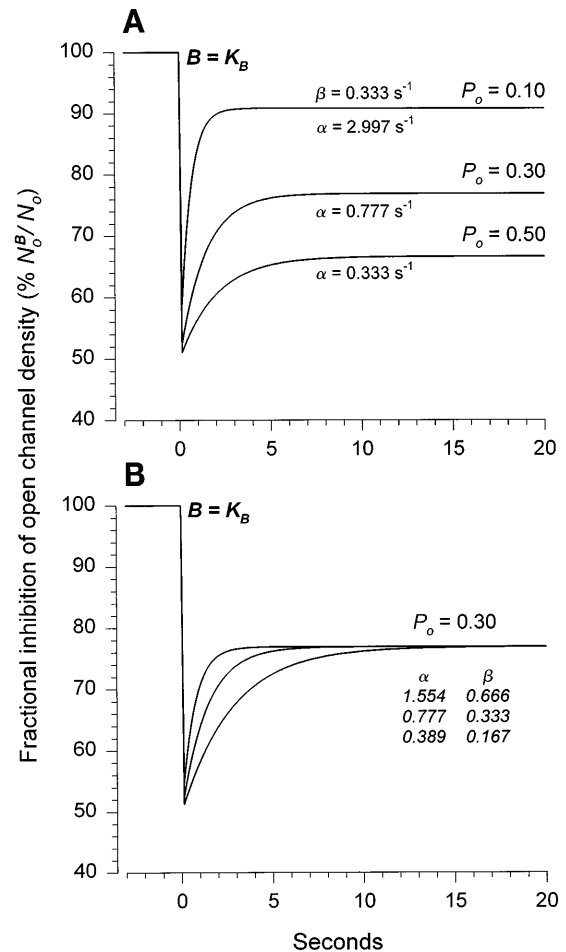


Fig. 1. Theoretical time rates of change of open channel density (expressed as fractional inhibition of open channel density) according to a 3-state model of closed, open, and blocked states in which blocker [6-chloro-3,5-diaminopyrazine-2-carboxamide (CDPC)] interacts only with open state of channel (2). Blocker on ( $k_{ob}$ ) and off ( $k_{bo}$ ) rate coefficients were assumed to be equal to  $7 \text{ s}^{-1} \cdot \mu\text{M}^{-1}$  and  $210 \text{ s}^{-1}$ , respectively, where the blocker equilibrium constant  $K_B = 30 \mu\text{M}$ . Time constants for redistribution of channels among closed, open, and blocked states and equilibrium value of fractional inhibition depend on open-to-closed ( $\alpha$ ) and closed-to-open ( $\beta$ ) rate coefficients.  $N_o^B$  and  $N_o$ , open channel density in presence and absence of blocker, respectively. A:  $\beta$  was assumed to be constant ( $0.333 \text{ s}^{-1}$ ; mean closed time of 3 s) and values of  $\alpha$  were 0.333, 0.777, and  $2.997 \text{ s}^{-1}$  (mean open times of 3, 1.287, and 0.334 s, respectively), with channel open probabilities ( $P_o$ ) of 0.5, 0.3, and 0.1, respectively. B: values of  $\alpha$  and  $\beta$  were chosen to give same  $P_o$  but variable time constants for redistribution of channels between closed, open, and blocked states. For epithelial  $\text{Na}^+$  channels with mean open and closed times of several seconds, redistribution of channels to equilibrium requires  $\sim 15$ – $20$  s following step increases of blocker concentration (B).

constant as assessed from fractional changes of  $N_o^B/N_o$  but may be associated with a range of relaxation times dictated by the actual mean open and closed times of the channels. For this to occur, however,  $\alpha$  and  $\beta$  must change identically.

Because unstirred layers at the apical surface of the cells and exchange of solutions within the experimental chambers prevent instantaneous changes of  $B$  at the channel sites, time-dependent changes of  $N_o^B$  will reflect not only redistribution of channels between closed, open, and blocked states but also the time constant for

exchange of the apical solution ( $\tau_{\text{chamber}}$ ). For infinitely well mixed chambers with  $\tau_{\text{chamber}}$  of between 1 and 4 s, illustrated in Fig. 2A, where  $B$  increases exponentially from 10 to 30  $\mu\text{M}$ , the equilibrium value of  $N_o^B$  is the same, although the transient approach to equilibrium may be complex (Fig. 2B). In practice, with chamber volumes of  $\sim 0.6$  ml (1) that are perfused continuously at flow rates of  $\sim 4$ – $6$  ml/min, the time required for complete exchange would fall into a range of roughly 20–40 s. Accordingly, our experiments were limited to measurements of fractional inhibitions of blocker-sensitive open channel densities and short-circuit currents at times consistent with equilibrium redistribu-

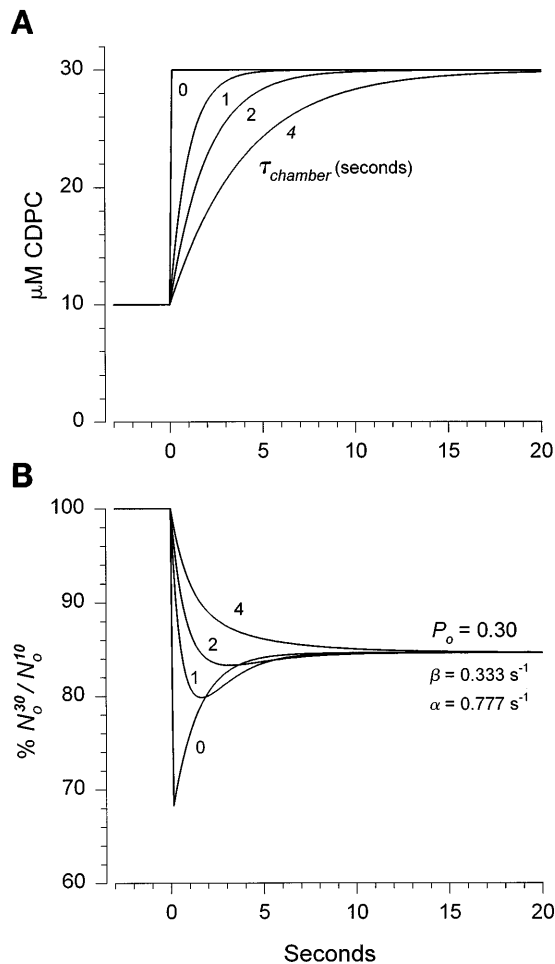


Fig. 2. *A*: theoretical calculations of influence of chamber mixing and exchange of solutions on time rate of increase of  $B$  as  $B$  is increased from 10 to 30  $\mu\text{M}$  at a constant flow rate. It was assumed that chambers are mixed infinitely well, with time constants for exchange of apical solution ( $\tau_{\text{chamber}}$ ) of 0, 1, 2, and 4 s. *B*: time rates of change of fractional inhibition of open channel density were calculated for channels with  $P_o$  of 0.3 and  $\tau_{\text{chamber}}$  of 0, 1, 2, and 4 s.  $N_o^{10}$  and  $N_o^{30}$ , open channel density in presence of 10 and 30  $\mu\text{M}$  CDPC, respectively. At slower perfusion rates relative to chamber volume, fractional inhibition of open channel density decreases monotonically as  $\tau_{\text{chamber}}$  becomes rate-limiting factor that determines time required for redistribution of channels to equilibrium at 30  $\mu\text{M}$  CDPC. Unstirred layers at apical surface of cells have not been taken into account in these calculations because their contribution to  $\tau_{\text{chamber}}$  is negligible relative to mixing and exchange time constants and because achieving infinitely well mixed compartments is unattainable in working with living tissues.

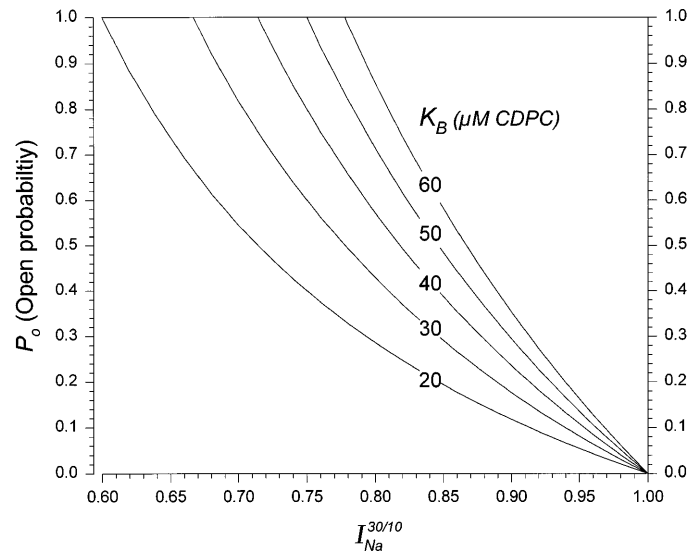


Fig. 3. Relationships between fractional inhibition of macroscopic blocker-sensitive short-circuit currents ( $I_{\text{Na}}^{30/10}$ ) and channel  $P_o$  at various  $K_B$  in response to increases of CDPC from 10 to 30  $\mu\text{M}$ .

tions of channels among closed, open, and blocked states.

*Graphic relationship between fractional inhibition of transport and the channel  $P_o$ .* Illustrated in Fig. 3 is the relationship between the fractional inhibition of blocker-sensitive  $\text{Na}^+$  entry into the cells caused by increasing  $B$  from 10 to 30  $\mu\text{M}$  CDPC at  $K_B$  ranging between 20 and 60  $\mu\text{M}$ . At a  $K_B$  of 30  $\mu\text{M}$ , blocker-sensitive  $\text{Na}^+$  entry would be inhibited by 15.4% if  $P_o$  is 0.3 ( $I_{\text{Na}}^{30/10} = 0.846$ ). Because short-circuit currents can be measured precisely and with high resolution ( $<0.01 \mu\text{A}/\text{cm}^2$ ), small changes of  $P_o$  can be resolved.

Our theory is predicated on the assumption that blockers interact solely with the open state of the channel, with the expectation that the concentration of blocker required to inhibit 50% of the macroscopic rate of transport ( $K_{\text{transport}}$ ) is greater than the  $K_B = k_{\text{bo}}/k_{\text{ob}}$  for interaction of the blocker with the open state of the channel. Consequently,  $K_{\text{transport}} = K_B/P_o$ . We know from our own studies that this is the case for ENaCs in both frog skin and A6 epithelia under a wide variety of transport rates and conditions of study. To our knowledge, this is the general case, without exception, when comparisons are made of macroscopic and microscopic blocker inhibition constants. Consequently, for  $P_o$  that range between 0.5 and 0.1, the  $K_{\text{transport}}$  would be two to five times greater than the  $K_B$  for blocker interaction between open and blocked states of the channel, provided that single-channel current and  $N_T$  remain constant.

## MATERIALS AND METHODS

*Cell culture.* Three groups of experiments (*groups 1, 2, and 3*) were done, with differences among groups in passage number, growth medium, and the permeabilized substrates on which the tissues were grown. Cells in *group 1* at passages 84–88 originated in B. L. Blazer-Yost's laboratory, where confluent tissues were grown on Transwell tissue culture treated inserts (Tr-tct, Costar, Cambridge, MA). Confluent

monolayers were brought to Urbana, IL, for the experimental part of the studies. Cells in *group 2* were purchased from the American Type Culture Collection at *passage 69*, subcultured, and used at *passage 73* with tissue growth on Millicell HA substrates (Millipore, Bedford, MA) in Urbana. Cells in *group 3* were obtained as a gift to W. J. Els from W. Van Driessche, used at *passages 108* with tissue growth on Millicell HA substrates, and studied in Cape Town, South Africa.

**Growth and perfusion media.** The growth medium for *group 1* experiments was a Dulbecco's modified Eagle's medium (91-5055EC; GIBCO, Grand Island, NY) with penicillin (25 U/ml) and streptomycin (25 µg/ml; GIBCO); 10% calf serum (CELLect, iron-supplemented calf serum, ICN Biomedicals, Aurora, OH) was added to this medium. Cells and tissues were maintained in a humidified incubator at 28°C with air containing 5.0% CO<sub>2</sub>. The tissues were studied on *days 14–26* after an overnight incubation in serum-free medium.

The growth medium for *group 2* and *group 3* experiments was a Dulbecco's modified Eagle's medium (84-5022EC, GIBCO) with 4 mM HEPES, 25 U/ml penicillin, 25 µg/ml streptomycin (BioWhittaker, Walkersville, MD), and 10% fetal bovine serum (Hyclone, Logan, UT). Cells and tissues were grown in the presence of humidified air containing 1% CO<sub>2</sub> in an incubator at 28°C.

**Electrical measurements and experimental protocol.** The methods of study with blocker-induced noise analysis were identical to those described in detail previously (10, 11, 14), except for the pulse protocol of exposure of the tissues to CDPC. After transfer to perfusion chambers designed for noise analysis (1), the tissues were short-circuited continuously for at least 1 h to allow the macroscopic short-circuit currents ( $I_{sc}$ ) to stabilize. The tissues were perfused with growth medium minus the fetal bovine serum and antibiotics.

Each tissue served as its own control with 2-h control periods and 6-h experimental periods during which the tissues were exposed to 2.7 µM aldosterone. About 30 min before the beginning of the control periods, 10 µM CDPC (Aldrich Chemical, Milwaukee, WI) was added to the apical perfusion solution; 10 µM CDPC caused an immediate small inhibition of the  $I_{sc}$  followed by an autoregulatory return of the short-circuit current at 10 µM CDPC ( $I_{sc}^{10}$ ) to the original value of  $I_{sc}$ . During control and experimental periods, the apical perfusion solution was switched at intervals of 20 min to the same solution containing 30 µM CDPC for pulse intervals of 3 min and returned thereafter to the 10 µM CDPC-containing solution. Values of  $I_{sc}^{10}$  and the currents in the presence of 30 µM CDPC ( $I_{sc}^{30}$ ) were recorded continuously on an analog strip-chart recorder and digitally at intervals of 10 s from digital meters before and during pulse inhibition of the short-circuit currents to assess the fractional inhibition of Na<sup>+</sup> transport ( $I_{Na}^{30/10}$ ) after subtraction of the amiloride-insensitive currents.

**Noise analysis and blocker rate coefficients.** Regardless of Na<sup>+</sup> channel blocker, including CDPC, corner frequencies ( $f_c$ ) of induced current noise Lorentzians vary linearly with  $B$  (15). Accordingly, the  $k_{ob}$  and  $k_{bo}$  can be determined from a two-point analysis, where  $2\pi f_c = k_{ob}B + k_{bo}$ . In the design of the pulse protocol presented here, it was convenient to expose the tissues chronically to 10 µM CDPC, since 1) this concentration of CDPC gave Lorentzians that could be analyzed reliably even at the lowest rates of transport (<1 µA/cm<sup>2</sup>), 2) switching between 10 µM and a single higher concentration of CDPC was sufficient to obtain all data required for determination of  $P_o$ , and 3) the differences of  $f_c$  at 30 and 10 µM CDPC ( $f_c^{30}$  and  $f_c^{10}$ , respectively) were sufficient to determine the blocker rate coefficients while minimally inhibiting

the short-circuit current to assure that single-channel currents remained practically constant at 10 and 30 µM CDPC (2).

Current noise measurements were made in pairs, at 10 µM CDPC before each pulse and after ~60 s of exposure to 30 µM CDPC. It became evident during these experiments (see *Blocker-dependent short-circuit currents*) that the autoregulatory increases of short-circuit currents in response to blocker inhibition of Na<sup>+</sup> entry were delayed by ~60–90 s, so that the fractional inhibitions of transport could be assessed before onset of autoregulatory changes of transport. Because  $f_c$  are independent of short-circuit current magnitudes, pairs of  $f_c^{30}$  and  $f_c^{10}$  at each pulse interval could be used to assess the time rates of change of the blocker rate coefficients and thus  $K_B$ .

Current noise was amplified after being filtered at the Nyquist frequency, digitized, and Fourier transformed to yield power density spectra. Low-frequency plateaus ( $S_0$ ) and  $f_c$  of the blocker-induced Lorentzians were determined by nonlinear curve fitting of the spectra to the Lorentzian, "1/ $f$ " noise at the lower frequencies and amplifier noise at the higher frequencies. The average of 60 2-s sweeps of current noise gave Lorentzians with uncertainty of  $f_c$  of  $\pm 1$  to  $\pm 2$  Hz. The sequential measurements of  $f_c^{10}$  and  $f_c^{30}$  were fit by nonlinear regression (TableCurve, Jandel Scientific) to smooth curves, thereby filtering small uncertainties in estimation of the blocker rate coefficients (see *CDPC rate coefficients*). The  $k_{ob}$  and  $k_{bo}$  were calculated from the slopes and intercepts of the rate-concentration plots ( $2\pi f_c = k_{ob}B + k_{bo}$ ) using the filtered  $f_c^{10}$  and  $f_c^{30}$  at 10 and 30 µM CDPC, respectively, and yielding  $K_B = k_{bo}/k_{ob}$ .

**Single-channel current and channel densities.** Blocker-insensitive Na<sup>+</sup> transport ( $I_{sc}^{amil}$ ) was measured at the end of each experiment by addition of 100 µM amiloride to the apical solution. Defining blocker-sensitive macroscopic currents ( $I_{Na}^B$ ) as  $I_{sc}^B - I_{sc}^{amil}$  and where  $S_0^0$  is  $S_0$  at 10 µM CDPC, the single-channel current through blocker-sensitive channels at a  $B_1$  of 10 µM CDPC is

$$i_{Na} = I_{Na}^{10} = \frac{S_0^0(2\pi f_c^{10})^2}{4 I_{Na}^{10} k_{ob} B_1} \quad (6)$$

since the  $i_{Na}$  in the absence of blocker is not significantly different from the  $i_{Na}^{10}$  (2). Blocker-sensitive open channel density at 10 µM CDPC is  $N_o^{10} = I_{Na}^{10}/i_{Na}^{10}$ , expressed in units of open channels per planar square centimeter or per 100 square micrometers, where the latter approximates the area per cell.  $N_o$  was calculated with *Eq. 2*. The total density of functional channels ( $N_T$ ) was calculated from the quotient  $N_o/P_o$ . It should be emphasized according to *Eq. 6* that all calculations of single-channel currents and channel densities were done with data obtained before onset of the blocker-related autoregulatory increases of transport, with the exception of the  $f_c^{30}$  that were used to calculate  $K_B$  and where, as noted above,  $f_c$  are independent of transport rate.

Summary data are reported as means  $\pm$  SE.

## RESULTS

**Blocker-dependent short-circuit currents.** Illustrated in Fig. 4 are the short-circuit current ( $I_{Na}^{10}$ ) responses to aldosterone in the three groups of experiments of markedly different baseline rates of transport. After a delay of ~40 min, the currents increased steadily over 6 h from baseline rates of  $1.06 \pm 0.11$  µA/cm<sup>2</sup> (*group 1*),  $5.40 \pm 0.37$  µA/cm<sup>2</sup> (*group 2*), and  $15.14 \pm 3.33$  µA/cm<sup>2</sup>

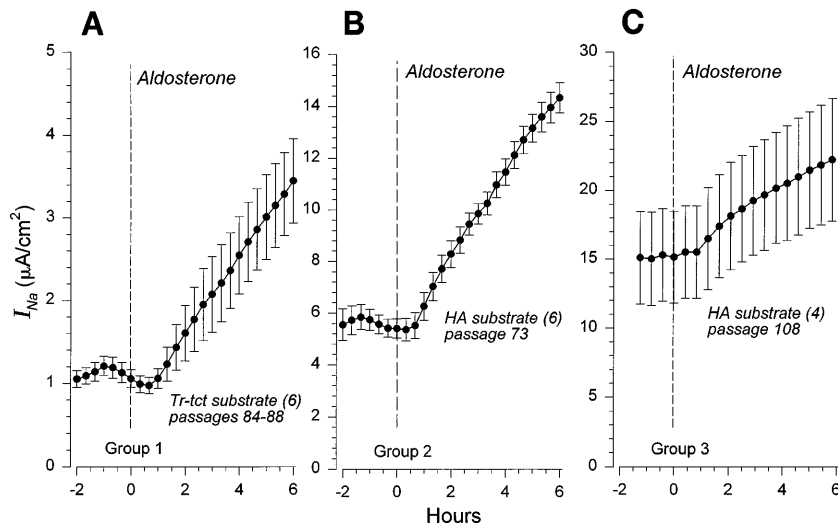


Fig. 4. Aldosterone stimulation of blocker-sensitive  $\text{Na}^+$  transport in tissue of groups 1, 2, and 3 (A, B, and C, respectively). Note differences in baseline rates of  $\text{Na}^+$  transport ( $I_{\text{Na}}$ ).

(group 3). The factors responsible for governing baseline rates of transport are unknown, although the substrate of tissue growth is of importance and is at least in part responsible for the very low rates of transport in group 1 tissues grown on Tr-tct membranes (16). Nevertheless, we were presented with the opportunity to test for similarities and differences in the responses to aldosterone at the earliest stages of stimulation of transport in tissues expressing vastly different rates of transport at the apical membranes of their cells.

Representative strip-chart recordings presented in Fig. 5 document the typical delay in onset of stimulation of  $I_{\text{sc}}$  caused by aldosterone and indicate the times at which CDPC was increased from 10 to 30  $\mu\text{M}$  and returned to 10  $\mu\text{M}$  CDPC. Although not the focus of the experiments, it was clearly apparent that the tissues responded with autoregulatory increases of  $I_{\text{sc}}$  in re-

sponse to inhibition of transport with transient overshoots of the  $I_{\text{sc}}$  following return to 10  $\mu\text{M}$  CDPC. The interesting point that emerged, as indicated in Fig. 6, was the delay in onset of the autoregulatory increase of  $I_{\text{sc}}$ . After the initial decline of the  $I_{\text{sc}}$  toward plateau values that persisted for  $\sim 20$ – $100$  s, the  $I_{\text{sc}}$  began to increase. This autoregulatory phenomenon has been reported previously and is associated with inhibition of transport resulting in long time constant transients of the  $I_{\text{sc}}$  in the range of 10–20 min (2, 14). Because the autoregulatory transients were clearly separable in time from the initial changes of  $I_{\text{sc}}$  caused by the blocker, the fractional inhibitions of  $I_{\text{sc}}$  could be calculated from the changes of  $I_{\text{sc}}$  at the plateaus before and  $\sim 30$ – $50$  s after elevation of CDPC to 30  $\mu\text{M}$ . For the pulses illustrated in Fig. 6, the fractional inhibitions ( $I_{\text{sc}}^{30/10}$ ) were 0.827, 0.861, and 0.879 at the respective  $I_{\text{sc}}$  of 1.68, 5.02, and 13.16  $\mu\text{A}/\text{cm}^2$ .

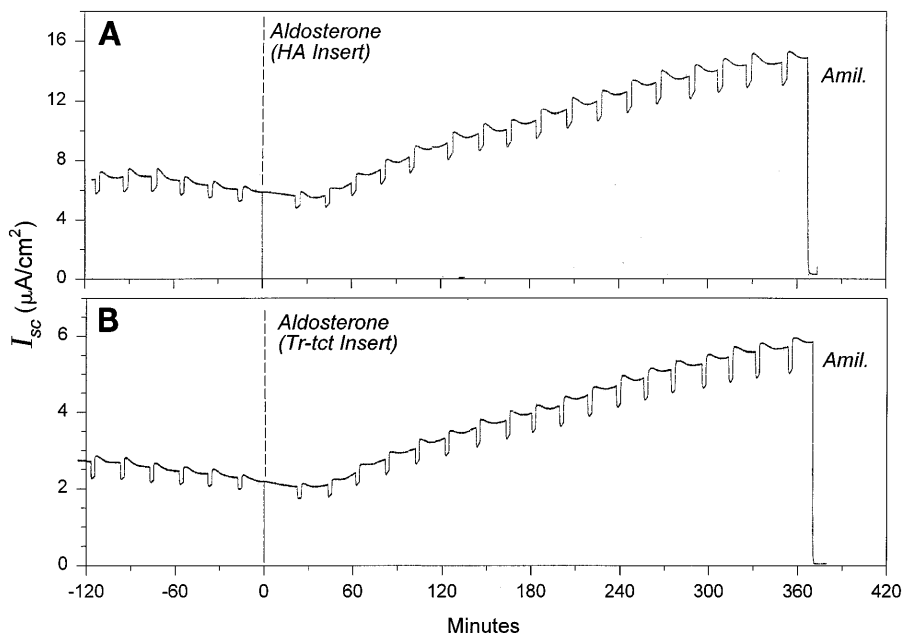
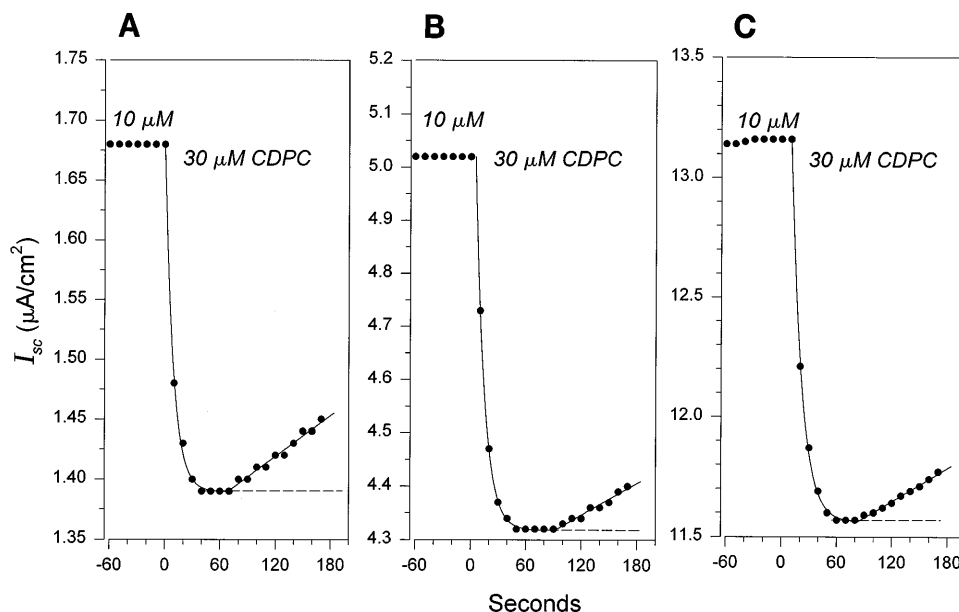


Fig. 5. Strip-chart recordings of short-circuit currents ( $I_{\text{sc}}$ ) during control periods and after treatment of tissues with aldosterone in A6 epithelia grown on HA (A) and Tr-tct (B) inserts.  $\text{Na}^+$  transport was inhibited by 100  $\mu\text{M}$  amiloride (Amil.) at ends of experiments. CDPC was increased from 10 to 30  $\mu\text{M}$  for 3 min at intervals of 20 min, causing pulse inhibitions of current.

Fig. 6. Measurements of fractional inhibition of  $\text{Na}^+$  transport in tissue of groups 1, 2, and 3 (A, B, and C, respectively). Values of  $I_{\text{sc}}$  were recorded at intervals of 10 s before and after increasing CDPC from 10 to 30  $\mu\text{M}$ . Dashed lines, plateau values at 30  $\mu\text{M}$  before onset of autoregulatory increases of transport. Note differences of baseline rates of  $\text{Na}^+$  transport and similar fractional inhibitions of  $I_{\text{sc}}$  caused by CDPC. See also completely reversible transient overshoots of  $I_{\text{sc}}$  in Fig. 5 following washout of 30  $\mu\text{M}$  CDPC and return to 10  $\mu\text{M}$  CDPC.



**CDPC rate coefficients.** Typical pairs of current noise-power density spectra are shown in Fig. 7 for tissues expressing very low (near 1  $\mu\text{A}/\text{cm}^2$ ; Fig. 7A) and higher rates of transport. Each pair of spectra yielded  $f_c^{10}$  and

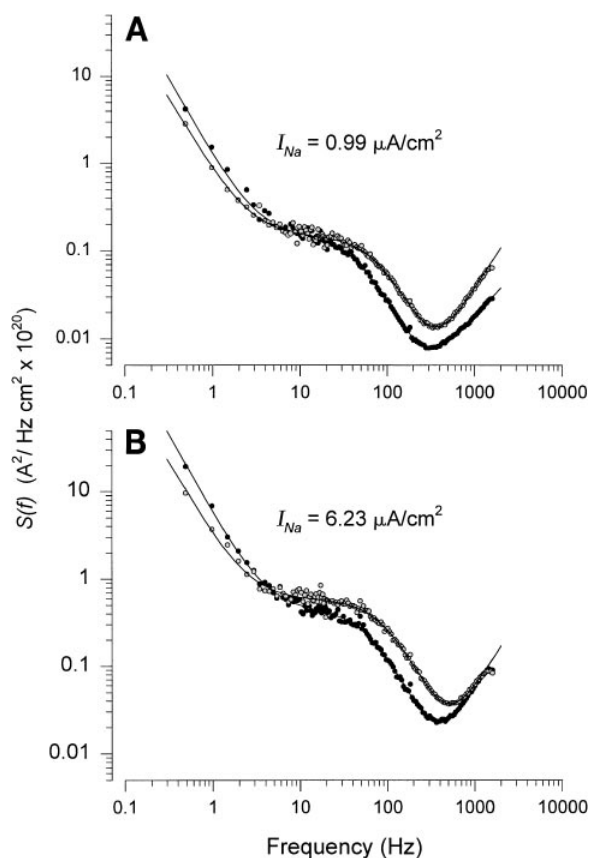


Fig. 7. Paired current noise-power density spectra  $[S(f)]$  at 10  $\mu\text{M}$  (solid circles) and 30  $\mu\text{M}$  CDPC (shaded circles) at low (A; 0.99  $\mu\text{A}/\text{cm}^2$ ) and intermediate (B; 6.23  $\mu\text{A}/\text{cm}^2$ ) rates of  $\text{Na}^+$  transport.  $f_c$ , Frequency. Corner frequencies ( $f_c$ ) were 47.3 and 75.3 Hz (A) and 60.9 and 89.5 Hz (B) at 10 and 30  $\mu\text{M}$  CDPC, respectively. Data were fit by nonlinear regression to 3 components, including a Lorentzian  $[S_0/[1+(f/f_c)^2]]$ , noise at low frequencies ( $S_1/f^\alpha$ ), and noise at higher frequencies ( $S_2 f^\beta$ ), originating at input stage of voltage amplifier.

$f_c^{30}$  together with their respective  $S_0$  values,  $S_0^{10}$  and  $S_0^{30}$ . As indicated in Fig. 8A, the  $f_c^{10}$  and  $f_c^{30}$  of a typical experiment were fit to smooth curves, thereby filtering the variance of  $f_c$  of individual measurements. The  $k_{\text{ob}}$ ,  $k_{\text{bo}}$ , and  $K_B$  were calculated at the respective times of measurement of the fractional inhibitions of  $I_{\text{sc}}$  (Fig. 8, B and C) with the projected values of  $f_c$  of the smooth curves.

In all groups of experiments, the mean  $K_B$  increased slightly and continuously during the 8-h periods of observation. As illustrated in Fig. 9, this was due to small increases of  $k_{\text{bo}}$  (Fig. 9B) and small decreases of  $k_{\text{ob}}$  in group 1 but not group 2 and 3 tissues (Fig. 9A). The changes of rate coefficients were, however, unrelated to aldosterone. The trends established during the control periods continued unchanged following exposure of the tissues to aldosterone. The zero time control values of  $k_{\text{ob}}$ ,  $k_{\text{bo}}$ , and  $K_B$  summarized in Table 1, determined just before addition of aldosterone to the apical solution, are similar to those reported previously, when  $k_{\text{ob}}$  and  $k_{\text{bo}}$  were determined from the linear relationship between the  $f_c$  measured over a larger range of CDPC concentrations (2). Accordingly, the channels recruited by aldosterone possess the same CDPC blocker kinetics as those present in the apical membrane before steroid stimulation of transport.

**Single-channel current and open-channel density.** Stimulation of  $\text{Na}^+$  transport by aldosterone could not be attributed to changes of single-channel current. Zero time control  $i_{\text{Na}}$  averaged 0.37, 0.30, and 0.27 pA in group 1, 2, and 3 tissues, respectively (Fig. 10), with corresponding open-channel densities of 3.1, 18.2, and 59.1 channels/100  $\mu\text{m}^2$  (Table 1). The  $i_{\text{Na}}$  remained practically constant during control and aldosterone treatment periods in group 1 and 2 tissues but was decreased significantly by aldosterone by  $\sim 10\%$  in group 3 tissues (Fig. 10). Accordingly, the changes of open-channel density (not shown),  $N_0 = I_{\text{Na}}/i_{\text{Na}}$ , paralleled those of  $I_{\text{Na}}$  from markedly different baseline values of  $N_0$ .

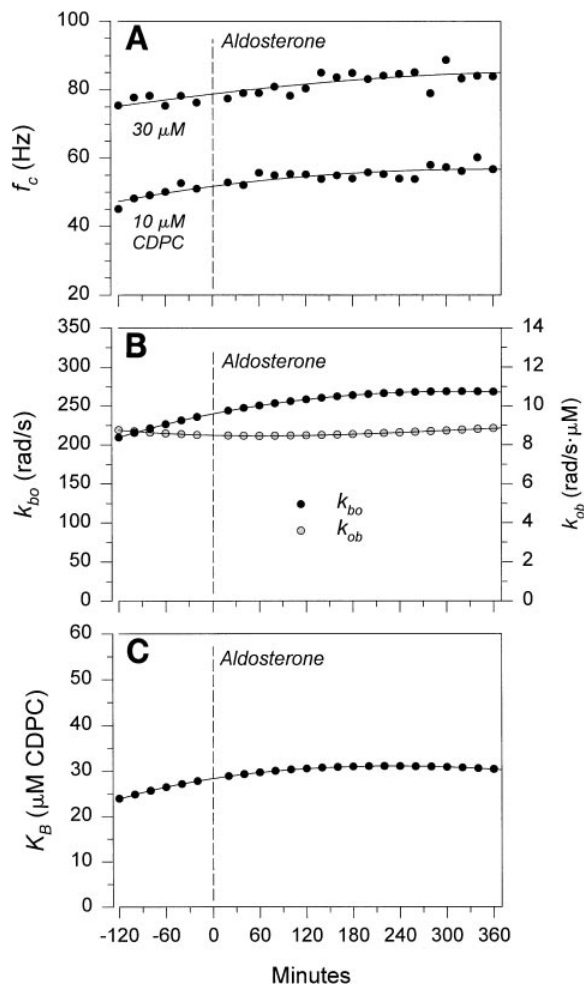


Fig. 8. Determination of CDPC blocker rate coefficients and  $K_B$ . *A*: pairs of  $f_c$  from a single experiment measured at 10 and 30  $\mu\text{M}$  CDPC as a function of time during control and experimental periods. Smooth curves were fit to data, and projected values on fitted curves were used to calculate  $k_{ob}$  and  $k_{bo}$  shown in *B*. rad, Radians. *C*: time-dependent changes of  $K_B = k_{bo}/k_{ob}$ . In the face of small random sampling errors in measurement of  $f_c$ , it is appropriate to filter or smooth data to best determine  $f_c$  at each time point. Given the simplicity of the data, we used TableCurve (Jandel Scientific) to fit simple curves, linear or nonlinear, to data points. More complex algorithms are available for data smoothing but were not required for data of present experiments.

**Channel open probability.** Stimulation of  $\text{Na}^+$  transport by aldosterone could not be attributed to changes of channel  $P_o$ . As indicated in Fig. 11*A* (and in normalized form in Fig. 11*B*),  $P_o$  fell slowly and progressively in *group 1* and *3* tissues during control and experimental periods and appeared to stabilize during the aldosterone treatment period in *group 2* tissues. When expressed as experimental values divided by zero time control values (Fig. 11*B*),  $P_o$  continued to fall ~20–25% after treatment of *group 1* and *3* tissues and to remain essentially unchanged in *group 2* tissues. Although we do not know the reason(s) for the chronic time-dependent decreases of  $P_o$ , it was evident that stimulation of transport could not be due to changes of channel  $P_o$  in any group of tissues, regardless of their baseline rates of transport or  $P_o$ . The zero time values of  $P_o$  averaged 0.44, 0.33, and 0.18 in *group 1*, *2*, and *3*

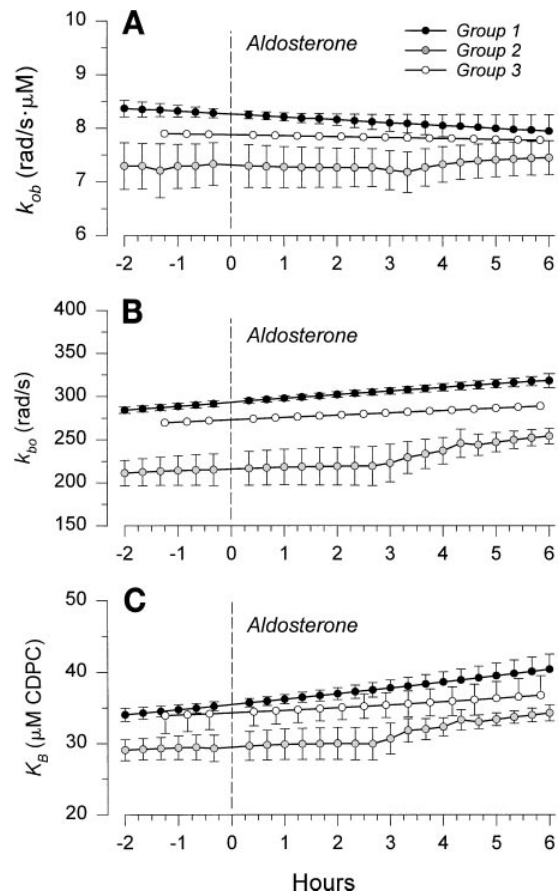


Fig. 9. Summary of time-dependent changes of  $k_{ob}$  (*A*),  $k_{bo}$  (*B*), and  $K_B$  (*C*) in *group 1*, *2*, and *3* tissues. Values are means  $\pm$  SE. Error bars were omitted for *group 3* for clarity of presentation.

tissues, respectively (Table 2), and appeared to be inversely related to the macroscopic  $I_{\text{Na}}$  (see *Dependence of  $P_o$  and  $N_T$  on macroscopic  $I_{\text{Na}}$* ).

**Functional channel densities.** Because stimulation of transport by aldosterone could not be attributed to changes of single-channel current or channel  $P_o$ , changes of transport must be due to increases of  $N_T$  ( $N_T \equiv$  channels in open and closed states) from baseline values of 10.9, 60.5, and 350 channels/100  $\mu\text{m}^2$  (Table 2). To compare changes of  $N_T$  and  $I_{\text{Na}}$  caused by aldosterone, the experimental values of  $N_T$  and  $I_{\text{Na}}$  were normalized to zero time control values as illustrated in Fig. 12. In *group 1* tissues expressing very low rates of transport,  $N_T$  was increased nearly fivefold within 6 h of treatment with aldosterone (Fig. 12*A*). The fractional increases of  $N_T$  were less in *group 2* and *3* tissues,

Table 1. Zero time baseline values of CDPC blocker rate coefficients and  $K_B$

	<i>n</i>	$k_{ob}$ , rad $\cdot$ s $^{-1}$ $\cdot$ $\mu\text{M}^{-1}$	$k_{bo}$ , rad/s	$K_B$ , $\mu\text{M}$
<i>Group 1</i>	6	7.30 $\pm$ 0.41	215.4 $\pm$ 19.0	29.5 $\pm$ 2.0
<i>Group 2</i>	6	8.26 $\pm$ 0.08	293.5 $\pm$ 2.5	35.5 $\pm$ 0.61
<i>Group 3</i>	4	7.88 $\pm$ 0.83	273.0 $\pm$ 40.1	34.3 $\pm$ 2.10

Values are means  $\pm$  SE; *n*, no. of observations. CDPC, 6-chloro-3,5-diaminopyrazine-2-carboxamide;  $k_{ob}$ , blocker on rate coefficient;  $k_{bo}$ , blocker off rate coefficient;  $K_B$ , blocker equilibrium constant; rad, radians.

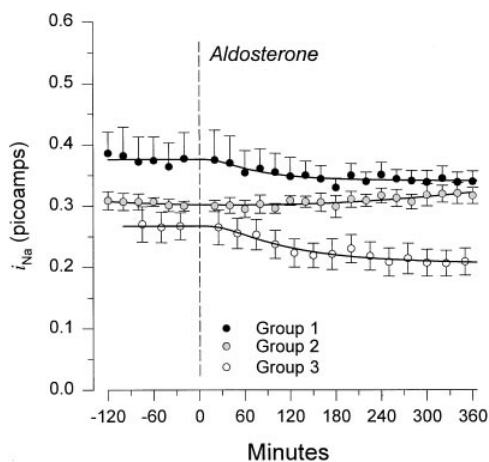


Fig. 10. Summary of time-dependent changes of single-channel currents ( $i_{Na}$ ) in *group 1*, *2*, and *3* tissues. Decreases of  $i_{Na}$  in *group 3* tissues after aldosterone are significant and are expected in tissues transporting  $Na^+$  at higher rates, where changes of apical membrane conductance lead to significant changes of fractional transcellular resistance and hence apical membrane voltage.

averaging near 2.8-fold (Fig. 12, *B* and *C*). The fractional increases of  $N_T$  in *group 1* and *3* tissues were greater than those of  $i_{Na}$ , due primarily to the chronic time-dependent decreases of  $P_o$  that occurred during the 6-h intervals that tissues were treated with aldosterone (Fig. 12, *A* and *C*), but were similar in *group 2* tissues, where the  $P_o$  had stabilized during this time (Fig. 12*B*). Although the fractional increases of  $N_T$  were largest in *group 1* tissues with very low baseline values of  $N_T$ , the largest absolute increases of  $N_T$  occurred in *group 3* tissues with the largest baseline values of  $N_T$ . Thus on average  $N_T$  (in channels/100  $\mu m^2$ ) was increased by aldosterone from  $10.9 \pm 3.0$  to  $43.5 \pm 9.0$  (*group 1*), from  $60.5 \pm 5.7$  to  $166 \pm 13.7$  (*group 2*), and from  $350 \pm 92$  to  $1,040 \pm 414$  (*group 3*).

Three additional tissues from *group 1* were treated overnight with aldosterone, after which time further changes of transport do not occur.  $i_{Na}$  averaged  $4.95 \pm 0.23 \mu A/cm^2$ ,  $i_{Na}$  averaged  $0.31 \pm 0.02$  pA,  $P_o$  averaged  $0.31 \pm 0.01$ , and  $N_T$  averaged  $56.0 \pm 4.5$  channels/100  $\mu m^2$ . When these values were compared with mean values obtained within 6 h of aldosterone treatment ( $3.45 \pm 0.51 \mu A/cm^2$ ,  $0.34 \pm 0.02$  pA,  $0.27 \pm 0.01$ , and  $43.5 \pm 9.0$  channels/100  $\mu m^2$ ), it was apparent that aldosterone exerted its major effects on  $Na^+$  transport and  $N_T$  within 6 h in these tissues.

**Dependence of  $P_o$  and  $N_T$  on macroscopic  $i_{Na}$ .** We noted previously (see *Channel open probability*) that  $P_o$  appeared to be inversely related to the macroscopic rates of  $Na^+$  transport in the absence of steroid treatment of the tissues. To examine this relationship in more detail, we plotted against  $i_{Na}$  (Fig. 13*A*) both the zero time control values of  $P_o$  and the values measured after 6-h periods of aldosterone stimulation of transport (Fig. 13*A*). Plotted also (Fig. 13*B*) are the zero time values of  $N_T$  and  $i_{Na}$  and those after stimulation by aldosterone. In both sets of data, a linear log-log relationship existed between  $P_o$  and  $i_{Na}$  and between  $N_T$  and  $i_{Na}$ . The regressions shown indicate the slopes and

99% confidence intervals. Over the range of  $i_{Na}$  between  $\sim 0.5$  and  $35 \mu A/cm^2$ ,  $P_o$  appears to decrease with increases of  $Na^+$  transport regardless of the presence or absence of aldosterone. Relative to the  $i_{Na}$ -related changes of  $N_T$  shown in Fig. 13*B*, changes of  $P_o$  are, however, relatively small, so that transport is determined primarily by changes of  $N_T$  whether caused by aldosterone and/or other factors that determine baseline rates of transport.

## DISCUSSION

From markedly different baseline rates of  $Na^+$  transport observed in the present studies and those reported in the literature, aldosterone stimulates transport severalfold regardless of the presence or absence of serum in the growth medium (4). For A6 epithelia treated chronically overnight with aldosterone, stimulation of transport has been attributed to increases of  $N_T$  with no measurable difference in  $P_o$  of the channels supporting baseline rates of transport from those recruited by aldosterone into the pool of channels responsible for blocker-sensitive  $Na^+$  entry into the cells (2). We arrive at the same conclusion for the present series of experiments in which increases of transport are mediated by

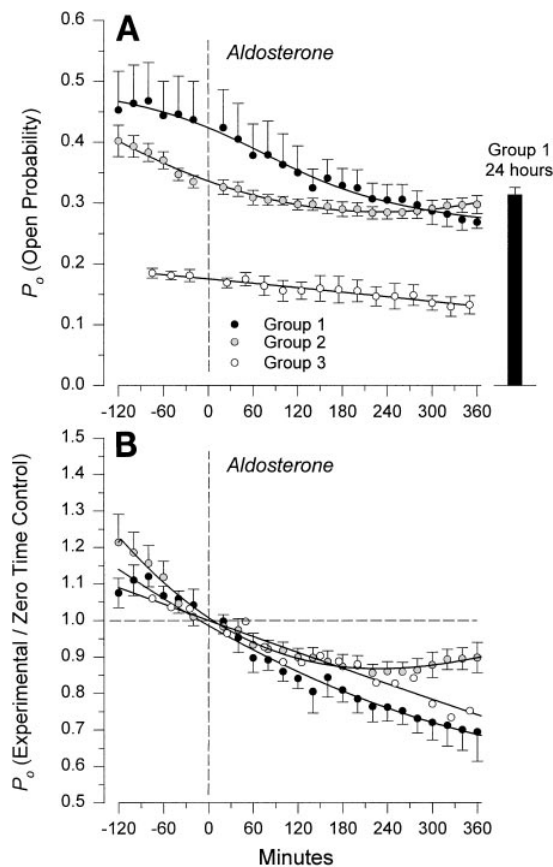


Fig. 11. Summary of time-dependent decreases of  $P_o$  in *group 1*, *2*, and *3* tissues. *A*: values are means  $\pm$  SE.  $P_o$  was also measured in *group 1* tissues 24 h after treatment with aldosterone (bar). *B*:  $P_o$  were normalized to interpolated zero time control values and expressed as experimental values/zero time control values (means  $\pm$  SE) for baseline-independent comparison of time rates of change of  $P_o$ . Error bars were omitted for *group 3* in *B* for clarity.

Table 2. Zero time baseline values

	<i>n</i>	$I_{sc}$ , $\mu\text{A}/\text{cm}^2$	$I_{Na}$ , $\mu\text{A}/\text{cm}^2$	$i_{Na}$ , pA	$N_o$ , channels/100 $\mu\text{m}^2$	$P_o$	$N_T$ , channels/100 $\mu\text{m}^2$
Group 1	6	$1.19 \pm 0.09$	$1.06 \pm 0.11$	$0.37 \pm 0.05$	$3.1 \pm 0.5$	$0.42 \pm 0.06$	$10.9 \pm 3.0$
Group 2	6	$5.60 \pm 0.38$	$5.40 \pm 0.37$	$0.30 \pm 0.01$	$18.2 \pm 1.6$	$0.33 \pm 0.01$	$60.5 \pm 5.7$
Group 3	4	$16.08 \pm 3.88$	$15.14 \pm 3.33$	$0.27 \pm 0.02$	$59.1 \pm 14.9$	$0.18 \pm 0.01$	$350 \pm 92$

Values are means  $\pm$  SE; *n*, no. of observations.  $I_{sc}$ , short-circuit current;  $I_{Na}$ , amiloride-sensitive  $I_{sc}$  ( $I_{Na} = I_{sc} -$  amiloride-insensitive  $I_{sc}$ );  $i_{Na}$ , single-channel current;  $N_o$ , open channel density ( $P_o N_T$ );  $P_o$ , open probability;  $N_T$ , channel density.

aldosterone or by other factors that govern baseline rates of transport. Regardless of baseline, aldosterone caused 2.8- to 5-fold increases of  $N_T$  within the first 6 h. The increases of  $N_T$  paralleled the increases of transport. Because single-channel currents either remained essentially constant at lower baselines of transport for which the fractional transcellular resistance approaches unity (*groups 1 and 2*) or decreased slightly, as is to be expected in tissues transporting  $\text{Na}^+$  at higher rates (*group 3*), there was no indication of either changes of single-channel conductance of the newly recruited channels or a major effect of aldosterone at the basolateral membranes that could have altered intracellular voltage and hence the single-channel currents.

We observed time-dependent decreases of  $P_o$  during the control periods that continued during the experimental periods after tissues were treated with aldosterone. Within the 6-h experimental periods,  $P_o$  stabilized only in *group 2* tissues (Fig. 11). Although the fractional decreases of  $P_o$  were relatively small ( $\sim 3$ –10%/h during control periods), it became apparent that these  $P_o$  transients required many hours for complete stabilization. When aldosterone-treated *group 1* tissues were studied the following day, their values of  $P_o$  were similar to those measured 6 h following treatment of tissues with aldosterone (Fig. 11A). Regardless of the

reason for such long-term transients during control and experimental periods, it was clearly apparent that aldosterone itself did not alter the  $P_o$  of the channels recruited to the pool of apical membrane channels subserving  $\text{Na}^+$  entry into the cells. In the face of decreasing or constant values of  $P_o$ , stimulation of transport by aldosterone must occur by increase of blocker-sensitive ENaC  $N_T$ .

It was also apparent over considerably larger ranges ( $\sim 70$ -fold) of transport than could be elicited by aldosterone (3- to 5-fold) that  $P_o$  was inversely related to  $\text{Na}^+$  transport, with the highest values of  $P_o$  observed at very low rates of transport (Fig. 11A). Transport-related decreases of  $P_o$  would be expected to be  $\sim 50\%$  per decade increase of  $I_{Na}$  or  $\sim 25\%$  per threefold increase of  $I_{Na}$ . Over any range of transport, it was nevertheless clear that  $P_o$  could vary substantially, due perhaps to a variety of factors involved in regulating  $P_o$  and unrelated to the direct action of aldosterone in stimulation of transport. Accordingly, over three- to fivefold consistent increases of transport caused by aldosterone, the aldosterone-related decreases of  $P_o$  would not be readily apparent and could be masked by other factors involved in regulation of  $P_o$ . Clearly,  $P_o$  is not constant, and it appears to vary with the rate of

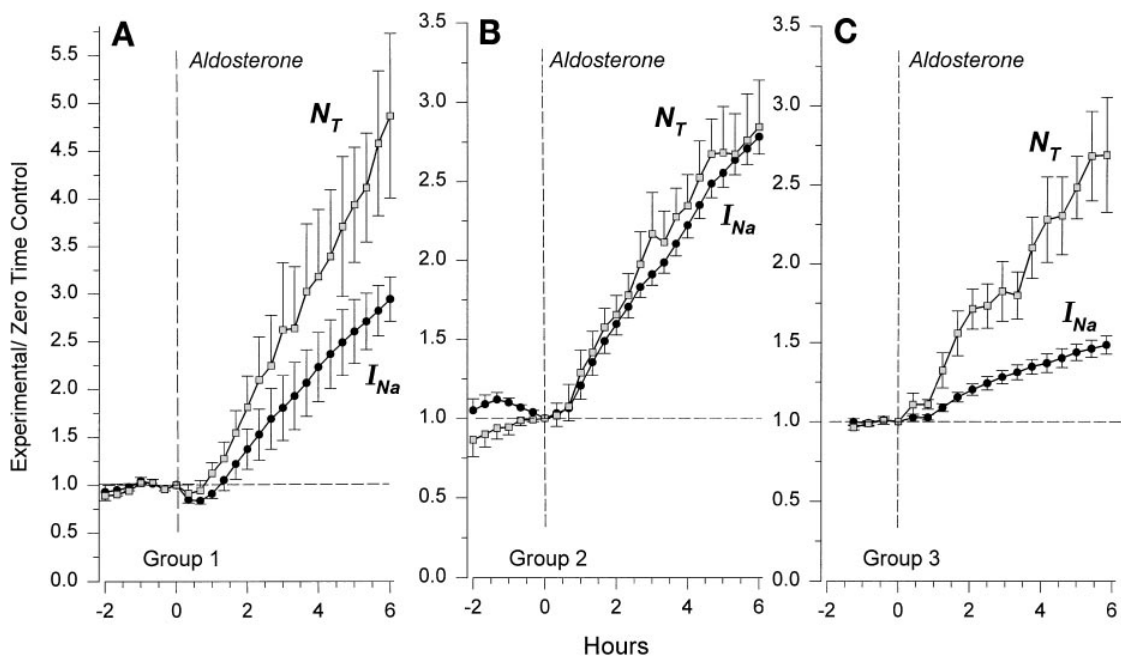


Fig. 12. Summary of time-dependent increases of channel density ( $N_T$ ) and blocker-sensitive  $\text{Na}^+$  transport ( $I_{Na}$ ) in *group 1, 2, and 3* tissues (A, B, and C, respectively). Values are means  $\pm$  SE expressed as experimental values/zero time control values.

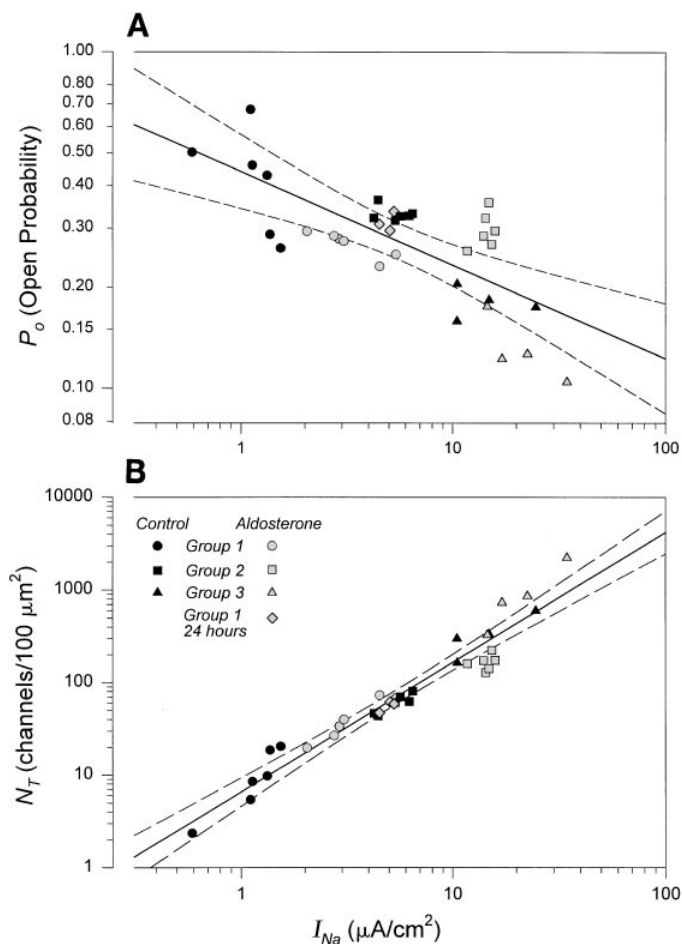


Fig. 13. Relationship between  $I_{Na}$  and  $P_o$  (A) and between  $I_{Na}$  and  $N_T$  (B). Zero time control values and paired values 6 h after treatment of group 1, 2, and 3 tissues with aldosterone are plotted. Scales are log-log. Solid lines, linear regressions; dashed lines, 99% confidence intervals.

$\text{Na}^+$  entry into the cells regardless of the presence or absence of aldosterone stimulation of transport.

Although it is well appreciated that A6 epithelia express baseline rates of transport that can vary enormously due to differences in growth media, serum, and other unknown factors, it has recently been shown that the substrate on which the cells are grown is a major determinant in expression of  $\text{Na}^+$  transport (16). Regardless of substrate and baseline rate of transport, all tissues respond to aldosterone, consistent with all reports in the literature. Although we attempted to diversify our experiments by use of different substrates and different growth media, it remains unknown whether the transport-related dependence of  $P_o$  is due solely to differences of apical membrane  $\text{Na}^+$  entry and/or to other factors associated with the substrate and the conditions of growth of the tissues. Nevertheless, regardless of the reasons for differences of baseline transport,  $N_T$  was directly related to transport rate both in the presence and absence of aldosterone stimulation of transport.

The modified pulse method used in the present studies has permitted for the first time a mechanically

noninvasive method of analysis of time-dependent changes not only of the blocker rate coefficients, single-channel currents, and open channel densities but also of the  $P_o$  and  $N_T$  of apical membrane ENaCs. Previous pulse method studies had indicated that  $P_o$  was independent of the fractional inhibition of open channel density (and hence fractional inhibition of  $I_{Na}$ ) over larger ranges of CDPC concentration than those used in the present studies (14).  $P_o$  has been shown to be independent of  $B$  and the time of exposure of the tissues to the blocker when studies were carried out with staircase protocol exposures to CDPC at concentrations exceeding 50  $\mu\text{M}$  (2, 10, 11, 13, 14). Chronic exposure of tissues to CDPC at their basolateral surface is without effect on short-circuit currents, indicating the nonresponsiveness of the cells to this agent if CDPC permeates the cells (unpublished observations). It is clear under all conditions so far studied that the effects of CDPC on transport are completely reversible regardless of the time of exposure of the tissues to this blocker. It is also quite apparent from the results of the present experiments compared with our own previous experiments with aldosterone (2) and those of others that the short-circuit current responses are the same regardless of the presence or absence of CDPC in the apical solution at comparable baseline rates of transport. Many blockers, including CDPC, have been used to characterize ENaCs, and there are to our knowledge no exceptions to the findings that blockers at any concentration do not alter the blocking site, as judged from the rate coefficients, and do not alter the single-channel conductance of the channel (17). Thus we know of no circumstance in which chronic exposure to 10  $\mu\text{M}$  CDPC would compromise the response of the tissues to hormonal stimulation by aldosterone in particular or to other drugs or hormones to which the responses are the same as those measured in the complete absence of CDPC (Refs. 25, 26; Blazer-Yost, Liu, and Helman, unpublished observations; Els, Liu, and Helman, unpublished observations). Accordingly, it should not be surprising that the results of the present studies are both qualitatively and quantitatively similar to previous reports that have used blocker-induced noise analysis as a way to study regulation of  $\text{Na}^+$  transport at the apical membranes of the cells, independent of the protocol used to analyze the tissues.

Our analysis has indicated that the principal mechanism underlying the early time-dependent increase of transport caused by aldosterone can be attributed to increase of the population density of blocker-sensitive ENaCs at the apical membranes of the cells with relatively little, if any, decrease of channel  $P_o$ .

We thank A. L. Helman for excellence in maintaining our tissue culture facility (Urbana, IL), the care and feeding of the cells, and assistance in the preparation of this manuscript.

This work was supported by National Institute of Diabetes and Digestive and Kidney Diseases Grant DK-30824 to S. I. Helman and also by a Department of Veterans Affairs merit review grant and an American Heart Association (Indiana Affiliate) grant-in-aid to B. L. Blazer-Yost.

X. Liu is a doctoral student in the Dept. of Molecular and Integrative Physiology, University of Illinois at Urbana-Champaign, Urbana, IL.

Address for reprint requests: S. I. Helman, Dept. of Molecular and Integrative Physiology, 524 Burrill Hall, 407 S. Goodwin Ave., University of Illinois at Urbana-Champaign, Urbana, IL 61801.

Received 5 August 1997; accepted in final form 3 December 1997.

## REFERENCES

- Abramcheck, F. J., W. Van Driessche, and S. I. Helman.** Autoregulation of apical membrane Na<sup>+</sup> permeability of tight epithelia. Noise analysis with amiloride and CGS 4270. *J. Gen. Physiol.* 85: 555–582, 1985.
- Baxendale-Cox, L. M., R. L. Duncan, X. Liu, K. Baldwin, W. J. Els, and S. I. Helman.** Steroid hormone-dependent expression of blocker-sensitive ENaCs in apical membranes of A6 epithelia. *Am. J. Physiol.* 273 (*Cell Physiol.* 42): C1650–C1656, 1997.
- Beron, J., and F. Verrey.** Aldosterone induces early activation and late accumulation of Na-K-ATPase at surface of A6 cells. *Am. J. Physiol.* 266 (*Cell Physiol.* 35): C1278–C1290, 1994.
- Bindels, R. J. M., J. M. Schafer, and M. C. Reif.** Stimulation of sodium transport by aldosterone and arginine vasotocin in A6 cells. *Biochim. Biophys. Acta* 972: 320–330, 1988.
- Broillet, M.-C., A. Berger, and J.-D. Horisberger.** Early effects of aldosterone on the basolateral potassium conductance of A6 cells. *Pflügers Arch.* 424: 91–93, 1993.
- Canessa, C. M., J. D. Horisberger, L. Schild, and B. C. Rossier.** Expression cloning of the epithelial sodium channel. *Kidney Int.* 48: 950–955, 1995.
- Canessa, C. M., L. Schild, G. Buell, B. Thorens, I. Gautschi, J.-D. Horisberger, and B. C. Rossier.** Amiloride-sensitive epithelial Na<sup>+</sup> channel is made of three homologous subunits. *Nature* 367: 463–466, 1994.
- Eaton, D. C., and Y. Marunaka.** Ion channel fluctuations: “noise” and single-channel measurements. In: *Channels and Noise in Epithelial Tissues*, edited by S. I. Helman and W. Van Driessche. San Diego, CA: Academic, 1990, p. 61–113. (*Curr. Top. Membr. Transp.*, vol. 37)
- Els, W. J., and S. I. Helman.** Activation of epithelial Na channels by hormonal and autoregulatory mechanisms of action. *J. Gen. Physiol.* 98: 1197–1220, 1991.
- Els, W. J., and S. I. Helman.** Dual role of prostaglandins (PGE<sub>2</sub>) in regulation of channel density and open probability of epithelial Na<sup>+</sup> channels in frog skin (*R. pipiens*). *J. Membr. Biol.* 155: 75–87, 1997.
- Granitzer, M., I. Mountian, and W. Van Driessche.** Effect of dexamethasone on sodium channel block and densities in A6 cells. *Pflügers Arch.* 430: 493–500, 1995.
- Helman, S. I., and L. M. Baxendale.** Blocker-related changes of channel density. Analysis of a three-state model for apical Na channels of frog skin. *J. Gen. Physiol.* 95: 647–678, 1990.
- Helman, S. I., and N. L. Kizer.** Apical sodium ion channels of tight epithelia as viewed from the perspective of noise analysis. In: *Channels and Noise in Epithelial Tissues*, edited by S. I. Helman and W. Van Driessche. San Diego, CA: Academic, 1990, p. 117–155. (*Curr. Top. Membr. Transp.*, vol. 37)
- Helman, S. I., and X. Liu.** Substrate-dependent expression of Na<sup>+</sup> transport and shunt conductance in A6 epithelia. *Am. J. Physiol.* 273 (*Cell Physiol.* 42): C434–C441, 1997.
- Helman, S. I., and W. Van Driessche (Editors).** *Channels and Noise in Epithelial Tissues*. San Diego, CA: Academic, 1990. (*Curr. Top. Membr. Transp.*, vol. 37)
- Horisberger, J.-D., and C. Kaufmann.** Early effects of aldosterone on apical and basolateral membrane conductances of TBM cells. *Am. J. Physiol.* 263 (*Cell Physiol.* 32): C384–C388, 1992.
- Kemendy, A. E., T. R. Kleyman, and D. C. Eaton.** Aldosterone alters the open probability of amiloride-blockable sodium channels in A6 epithelia. *Am. J. Physiol.* 263 (*Cell Physiol.* 32): C825–C837, 1992.
- Leal, T., and J. Crabbé.** Effects of aldosterone on (Na<sup>+</sup>+K<sup>+</sup>)-ATPase of amphibian sodium-transporting epithelial cells (A6) in culture. *J. Steroid Biochem.* 34: 581–584, 1989.
- Ling, B. N., and D. C. Eaton.** Effects of luminal Na<sup>+</sup> on single Na<sup>+</sup> channels in A6 cells, a regulatory role for protein kinase C. *Am. J. Physiol.* 256 (*Renal Fluid Electrolyte Physiol.* 25): F1094–F1103, 1989.
- Marunaka, Y., and D. C. Eaton.** Effects of vasopressin and cAMP on single amiloride-blockable Na channels. *Am. J. Physiol.* 260 (*Cell Physiol.* 29): C1071–C1084, 1991.
- Pacha, J., G. Frindt, L. Antonian, R. B. Silver, and L. G. Palmer.** Regulation of Na channels of the rat cortical collecting tubule by aldosterone. *J. Gen. Physiol.* 102: 25–42, 1993.
- Palmer, L. G., L. Antonian, and G. Frindt.** Regulation of the Na-K pump of the rat cortical collecting tubule by aldosterone. *J. Gen. Physiol.* 102: 43–57, 1993.
- Paunescu, T. G., and S. I. Helman.** Dual role of prostaglandin E<sub>2</sub> in regulation of Na<sup>+</sup> transport in A6 epithelia (Abstract). *Biophys. J.* 72: A230, 1997.
- Paunescu, T. G., X. Liu, and S. I. Helman.** Nonhormonal regulation of apical membrane sodium transport in A6 epithelia (Abstract). *FASEB J.* 11: A8, 1997.
- Shahedi, M., K. Laborde, L. Bussi eres, and C. Sachs.** Acute and early effects of aldosterone on Na-K-ATPase activity in Madin-Darby canine kidney epithelial cells. *Am. J. Physiol.* 264 (*Renal Fluid Electrolyte Physiol.* 33): F1021–F1026, 1993.
- Verrey, F., and J. Beron.** Activation and supply of channels and pumps by aldosterone. *News Physiol. Sci.* 11: 126–133, 1996.